Advanced Performance Materials 4, 9–23 (1997)

Influence of the Heat Treatments on Creep Behaviour of Nickel Aluminide with Boron

A.M. HASHEM
Faculty of Eng. & Tech., Minia University, Minia 61111, Egypt

D. STOVER AND H.-P. BUCHKREMER
IAW, Forschungszenttrum Julich, Germany

E. EL-MAGD
LFW/ RWTH Aachen, Germany

Abstract. The nickel aluminide with boron alloy is being considered for elevated-temperature structural application in particular for jet turbine engine components. The alloy is attractive due to its ease of production, the low cost of its components, and its property advantages relative to superalloys. Therefore, if alloys based on Ni_3Al are successfully developed, substantial increases in engine performance and efficiency may be realized.

The creep characteristics of an intermetallic Ni_3Al alloy containing boron produced by hot isostatic pressing were investigated in the temperature range 800 to 900°C. Various heat treatments were used to produce different initial grain sizes of this alloy.

Parameters studied were steady state strain rate, time to fracture, ductility and Larson-Miller parameter. The stress exponent, activation energy for creep and grain size exponent were calculated.

It was found that by increasing the temperature of the heat treatment, the grain size increased. The results showed that the creep behaviour for this alloy improved as grain size increased. Furthermore, a comparison of the resulting creep data with data obtained from references is discussed.

Keywords: creep properties, grain size, heat treatment, nickel aluminide with boron

1. Introduction

Ordered intermetallic alloys constitute a unique class of metallic materials which form long-range ordered crystal structure below their melting points (T_m) [1]. Among these intermetallic compounds, nickel aluminide (Ni_3Al) with $L1_2$ structure, one of the main constituents in nickel superalloys, has useful characteristics for a resistant material. It has been known for many years that Ni_3Al (γ'-phase) exhibits the unusual property of increased yield strength with increasing temperature up to 800°C [1–3]. The structures and properties of ordered intermetallic alloys were studied extensively in the 1950's to 1960's, and as a result of these efforts many properties were identified and characterized [3].

The recent discovery that polycrystalline Ni_3Al can be rendered ductile by microalloying with boron has resulted in a great advance in development of such alloys. Akoi and Izumi [4] first discovered the beneficial effect of boron in Ni_3Al and observed that the tensile ductility of Ni_3Al with boron was about 35 percent at room temperature, while for Ni_3Al

without boron, the ductility was less than 5 percent. With control of the boron concentration and thermomechanical treatment, Liu and Kock [5] obtained tensile elongations exceeding 50 percent for boron-doped Ni_3Al containing 24 atom percent Al.

The ordered intermetallic compound Ni_3Al alloy is used for a range of structural applications. These include gas and steam turbines, aircraft fasteners, gas and oil well tubular products, components for corrosive environments, heating elements for a range of appliances, and automotive pistons, turbochargers and valves [6]. However, for successful use of intermetallic alloys, the development of their processing technology and properties is still required.

This research studies the effect of boron addition to Ni_3Al on the creep behaviour at elevated temperatures. This alloy was produced by a hot isostatic pressing (HIP) technique. Various heat treatments were used to produce a wide range of initial grain size. Creep behaviour has been studied in the temperature range of 800 to 900°C at different stress levels. The influence of the various heat treatments on the creep properties were investigated. Furthermore, comparison between creep behaviour of the present alloy and that found in Ref. [7] is made.

2. Materials and procedures

2.1. Material

The chemical composition of the alloy was 76 at.% Ni, 24 at.% Al and 0.5 at.% B. The alloy was produced by hot isostatic pressing (HIP) in KFA Julich (Germany) under the conditions 1250°C/2000 bar/4 hours. Figure 1(a) shows a micrograph of the initial grain size of the alloy.

2.2. Heat treatment

The conditions of different heat treatments and corresponding grain sizes obtained are listed in Table 1. All specimens were air cooled after heat treatments. Figure 1 shows micrograph of the alloy at different heat treatments. It can be seen that increasing the temperature of the heat treatment increases the grain size.

Table 1. Conditions of heat treatments and values of grain size.

Heat treatments	Parameters	Grain size (d) [μm]
WHT	as received	20.27
HT1	1000 C/24 hours	21.05
HT2	1120 C/4 hours	101.5
HT3	1250 C/90 min.	106.0

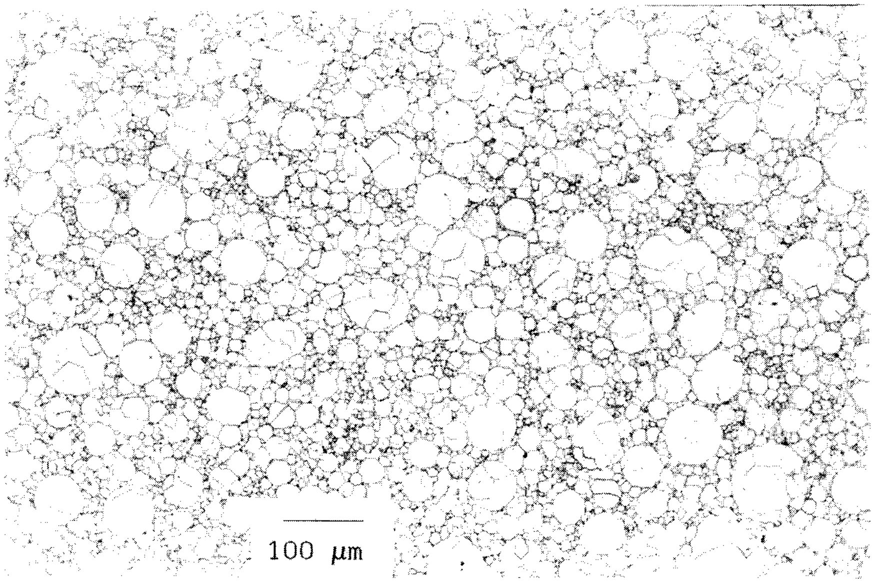

(a)

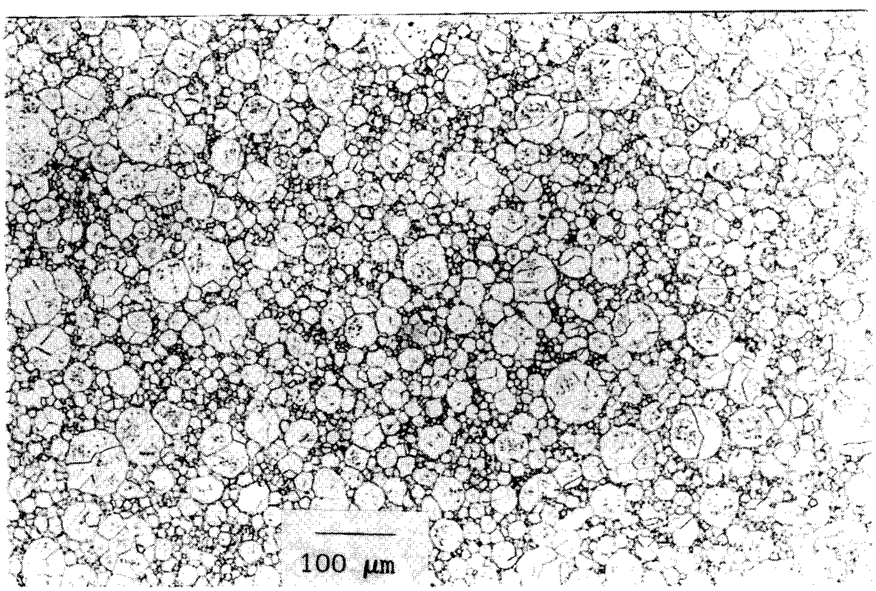

(b)

Figure 1. Initial micrographs of grain size for different heat treatments: (a) WHT, NI_3Al + 0,5 at.% B, V = 100*x*, (b) HT1, 1000°C/24 h/air, (c) HT2, 1120°/4 h/air, (d) HT3, 1250°C/1.5 h/air.

(*Continued on next page*)

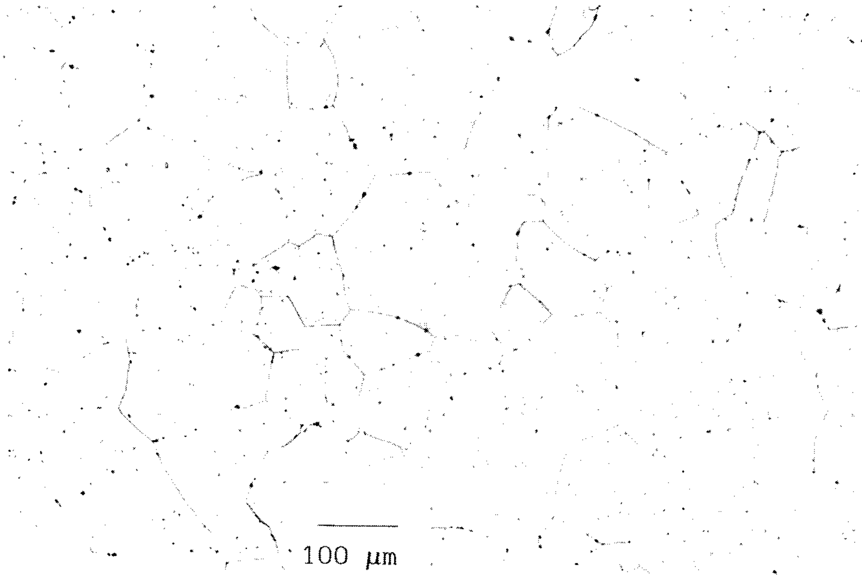

(c)

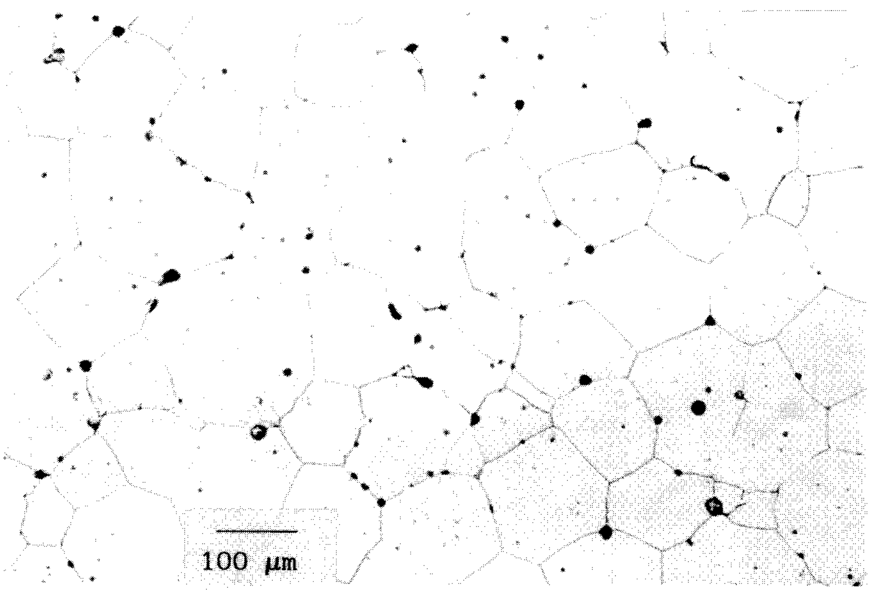

(d)

Figure 1. (*Continued*.)

2.3. Creep specimen

Creep specimens were cylindrical rods of 50 mm total length having a threaded head M8 of 8 mm length on each side. The gauge diameter was 4.5 mm and the gauge length was 25 mm.

2.4. Creep test procedure

Creep tests were carried out according to standard DIN 50118. The creep load was applied smoothly at the beginning of the test. All creep tests were continued to fracture.

The creep tests were carried out on a 12 kN creep testing constant load machine. The temperature was measured using Cr-Ni thermocouple and was controlled by an automatic control system to keep the test temperature to within ±0.5°C.

Readings of elongation were recorded using a high-sensitive extensometer. More frequent readings were recorded during the early part of the test than at later stages. Creep strain was measured with a resolution of $\varepsilon \cong 10^{-6}$, which allows an accurate determination of creep behaviour.

3. Results and discussions

3.1. Creep data

All the creep tests were carried out in air at temperatures of 800, 850 and 900°C under various levels of engineering stress. A typical creep curve is presented in figure 2. Steady state strain rate ($\dot{\varepsilon}_{ss}$), time to fracture (t_f), percentage elongation at fracture (A%) and Larson-Miller parameter (L-M) were determined from each creep test (Table 2).

The creep behaviour obtained in the entire stress range of the investigation exhibit a very similar to that high temperature alloys, yielding a primary, secondary and tertiary creep stage.

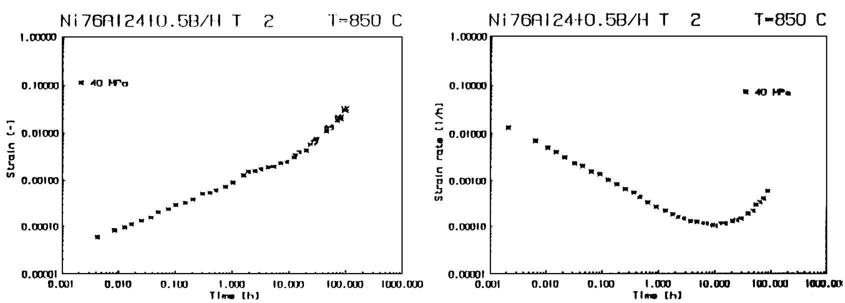

Figure 2. A typical creep curve e.g., HT2 at 40 MPa and 850°C.

Table 2. Creep properties of Ni_3Al for different heat treatments.

Heat treatment	Temperature [°C]	Stress [MPa]	Min. strain rate [1/h]	Time to fracture [h]	Elongation [%]	L-M parameter $*10^3$
WHT	800	90,0	$9{,}46{\cdot}10^{-3}$	0,767	1,00	21,34
	800	70,0	$3{,}00{\cdot}10^{-3}$	3,700	2,37	22,07
	800	50,0	$1{,}50{\cdot}10^{-3}$	17,330	5,61	22,60
	800	40,0	$1{,}00{\cdot}10^{-3}$	49,030	7,94	23,27
	800	20,0	$1{,}20{\cdot}10^{-4}$	1150,000	12,50	24,74
HT1 1000°C/24 h	800	90,0	$9{,}00{\cdot}10^{-3}$	1,217	2,26	21,55
	800	80,0	$5{,}80{\cdot}10^{-3}$	2,333	2,86	21,85
	800	60,0	$2{,}90{\cdot}10^{-3}$	7,100	4,83	22,37
	800	50,0	$1{,}60{\cdot}10^{-3}$	15,570	5,55	22,74
	800	40,0	$8{,}60{\cdot}10^{-4}$	21,933	7,60	22,90
	800	20,0	$6{,}40{\cdot}10^{-5}$	981,833	19,86	24,70
HT2 1200°C/4 h	800	70,0	$2{,}70{\cdot}10^{-4}$	14,533	0,80	22,70
	800	60,0	$7{,}00{\cdot}10^{-5}$	41,067	2,37	23,77
	800	50,0	$4{,}00{\cdot}10^{-5}$	295,040	2,90	24,10
	800	45,0	$2{,}00{\cdot}10^{-5}$	402,390	3,43	24,25
	850	60,0	$6{,}00{\cdot}10^{-4}$	10,583	1,30	23,60
	850	50,0	$3{,}60{\cdot}10^{-4}$	48,750	2,38	24,35
	850	40,0	$1{,}00{\cdot}10^{-4}$	102,867	3,95	24,72
	850	30,0	$6{,}00{\cdot}10^{-5}$	224,833	4,62	25,10
	900	55,0	$1{,}00{\cdot}10^{-3}$	6,100	1,59	24,40
	900	50,0	$9{,}00{\cdot}10^{-4}$	11,467	2,44	24,70
	900	40,0	$5{,}50{\cdot}10^{-4}$	19,467	3,57	24,97
	900	30,0	$1{,}50{\cdot}10^{-4}$	43,317	3,90	25,38
HT3 1250°C/90 min.	800	60,0	$1{,}40{\cdot}10^{-4}$	92,250	2,96	23,57

3.2. Steady state creep characteristics

In high temperature creep, it is usual to express the secondary creep rate (steady state strain rate) by the Norton and Bailey equation [8]. The more general form of the constitutive equation, which includes grain size, is [9]

$$\dot{\varepsilon} = a(b/d)^p(\sigma/E)^n \exp(-Q/RT), \tag{1}$$

By the aid of this equation, stress exponent (n) the apparent activation energy for creep (Q) and grain size exponent (p) can be determined experimentally using the following expressions

$$n = (\delta \ln \dot{\varepsilon}_s / \delta \ln \sigma)_{T,d} \tag{2}$$
$$Q = -R(\delta \ln \dot{\varepsilon}_s / \delta(1/T))_{\sigma,d} \tag{3}$$
$$p = (\delta \ln \dot{\varepsilon}_s / \delta \ln(1/d))_{T,\sigma} \tag{4}$$

Table 3. Stress exponent and apparent activation energy of Ni_3Al with boron for different heat treatments.

Heat treatments	Temperature °C T	Stress exponent n	Activation energy (Q) kJ/mol 40	50 MPa
WHT	800	2.8 ± 0.2	—	—
HT1	800	3.2 ± 0.1	—	—
HT2	800	5.5 ± 0.8		
	850	3.5 ± 0.6	401 ± 15	328 ± 69
	900	3.2 ± 0.5		
HT3	800	—	—	—

Table 4. Grain size exponent for different heat treatments at creep test temperature 800°C.

Heat treatments	Grain size exponent (p) 40	60 MPa
WHT		
HT1		
HT2	2.73 ± 0.1	2.33 ± 0.1
HT3		

From the creep data obtained, the stress exponent and apparent activation energy were calculated and values are given in Table 3. Calculation for grain size exponent is given in Table 4.

3.3. Effect of test temperatures

3.3.1. Steady state strain rate. Figure 3 shows the relationship between the steady state strain rate and the applied stress for heat treatment 2 (HT2) at three test temperatures. According to Eq. (2) the stress exponent for temperatures 800, 850 and 900°C were 5.5, 3.84 and 3.15 respectively.

The temperature dependence on the steady state strain rate for HT2 at constant applied stresses is shown in figure 4. The apparent activation energies for creep as determined from the slopes of these plots are given in Table 3. It can be seen that the mean apparent activation energy of this alloy is 400 ± 15 kJ/mol at 40 MPa and 328 ± 69 kJ/mol at 50 MPa. Since no test was carried out at 40 MPa for HT2, the value of steady state strain rate for this condition was extrapolated from figure 3 and found equal to $1.2 * 10^{-5}$ 1/hour. The resulting activation energies were found higher than those for self-diffusion and solid solution of nickel alloys (280 to 305 kJ/mol) [10], but similar to the values reported for other nickel base superalloys and nickel aluminide (390 to 420 kJ/mol) [8, 10].

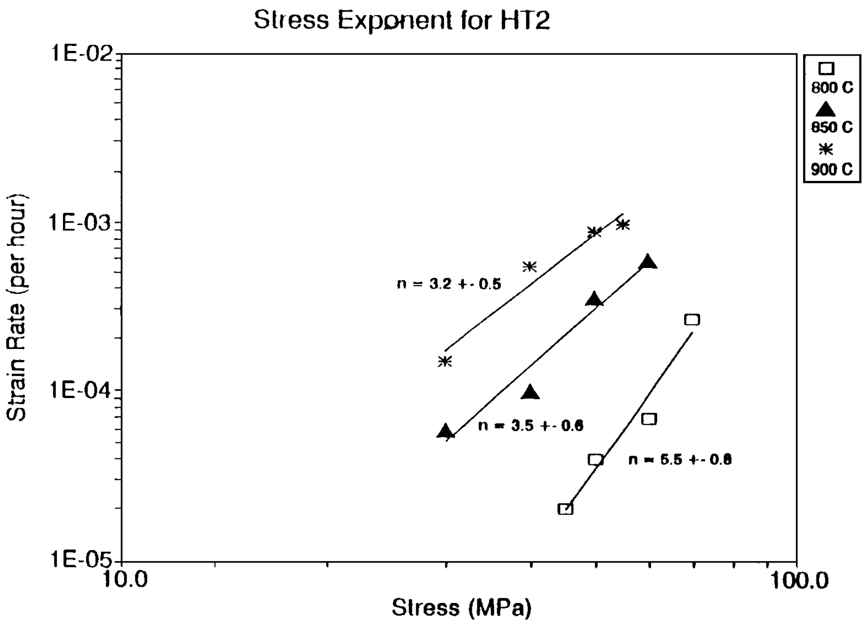

Figure 3. Steady state strain rate vs. applied engineering stress for HT2 and different test temperatures.

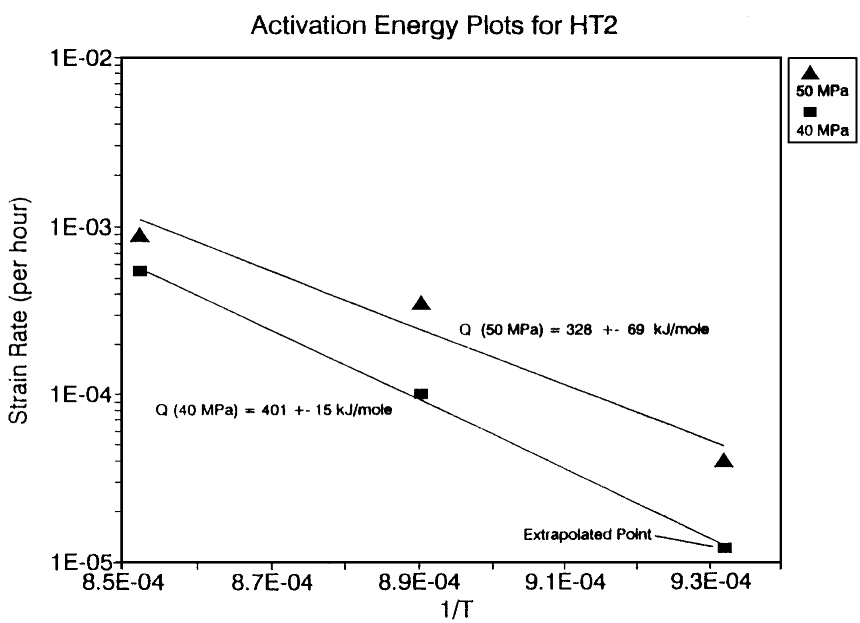

Figure 4. Steady state strain rate vs. $1/T$ for HT2. *Note:* Steady state strain rate at 40 MPa is extrapolated from figure 3.

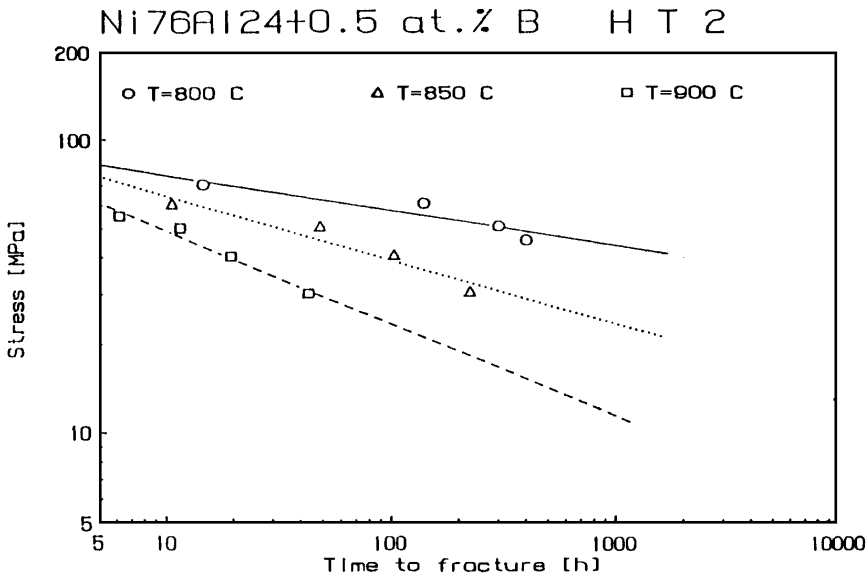

Figure 5. Applied engineering stress vs. time to fracture for HT2 and different test temperatures.

3.3.2. Time to fracture. The dependence of time to fracture on creep engineering stress for HT2 is shown in figure 5. These values for different temperatures are given in Table 2. Time to fracture ranged from 6.1 to 410 hours.

3.3.3. Ductility. Figure 6 shows the influence of the creep engineering stress on the percentage elongation for different test temperatures. The elongations at creep fracture are relatively low, having values of 0.8–3.5%, 1.3–4.6% and 1.6–4.0% at temperatures of 800, 850 and 900°C respectively. From these values it can be seen that the creep ductility increases with increasing the time to fracture. This can be attributed to the decrease of the applied stress.

3.4. Effect of heat treatments

3.4.1. Steady strain rate. Figure 7 shows the relationship between steady state strain rate and the applied engineering stress for different heat treatments at temperature of 800°C. It can be seen from this figure that no change in creep behaviour was detected for either WHT and HT1. However, the creep behaviour was greatly improved for both HT2 and HT3.

The stress exponents were 2.8 and 3.2 at a temperature of 800°C for WHT and HT1 respectively. That means, the extent of the secondary stage is less pronounced for this alloy ($n \cong 2$–5) than for a nickel base superalloy ($n \cong 8$–12).

The steady state strain rate as a function of grain size is shown in figure 8. The grain size exponents were determined from the slopes of these plots at a constant temperature of 800°C and stresses of 40 and 60 MPa. These values are listed in Table 4.

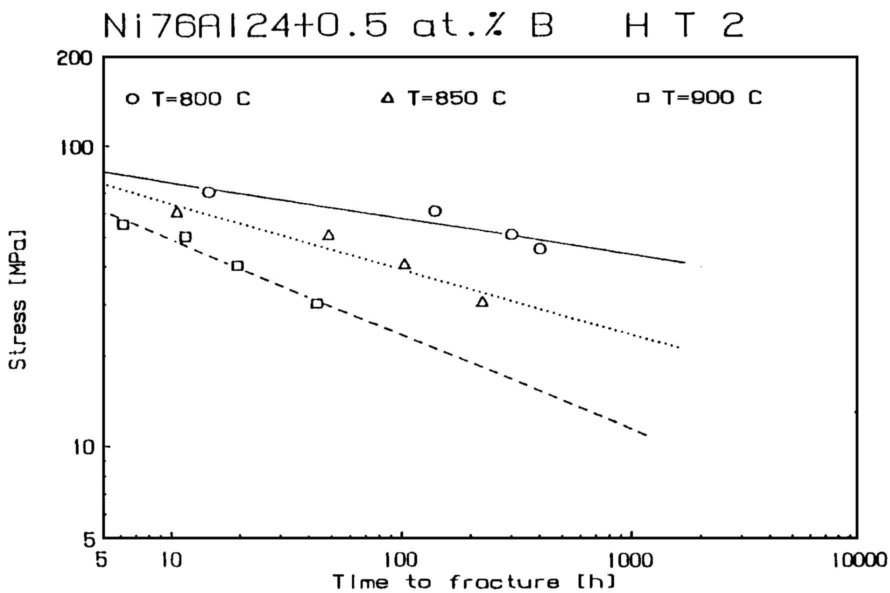

Figure 6. Percentage elongation at fracture vs. time to fracture for HT2 and different test temperatures.

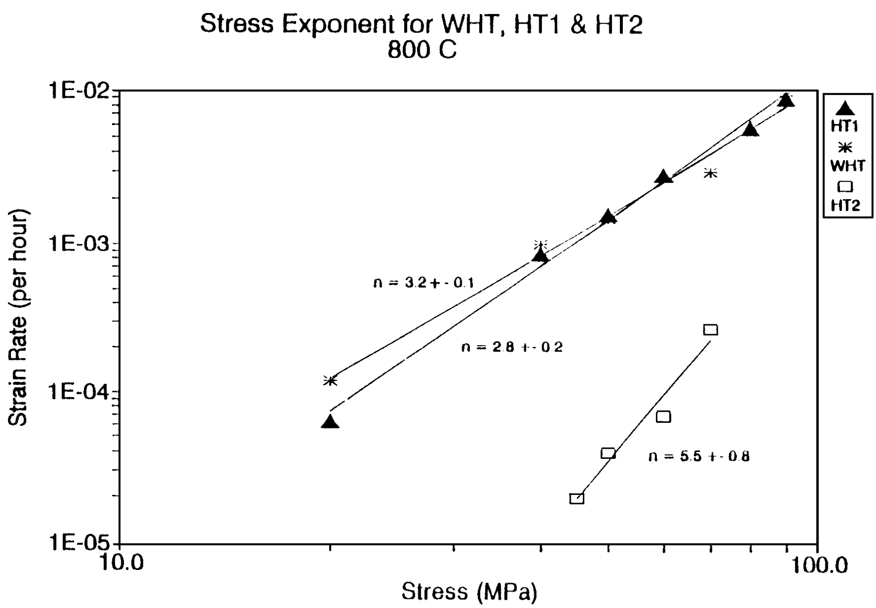

Figure 7. Steady state strain rate vs. applied engineering stress for different heat treatments and $T = 800°C$.

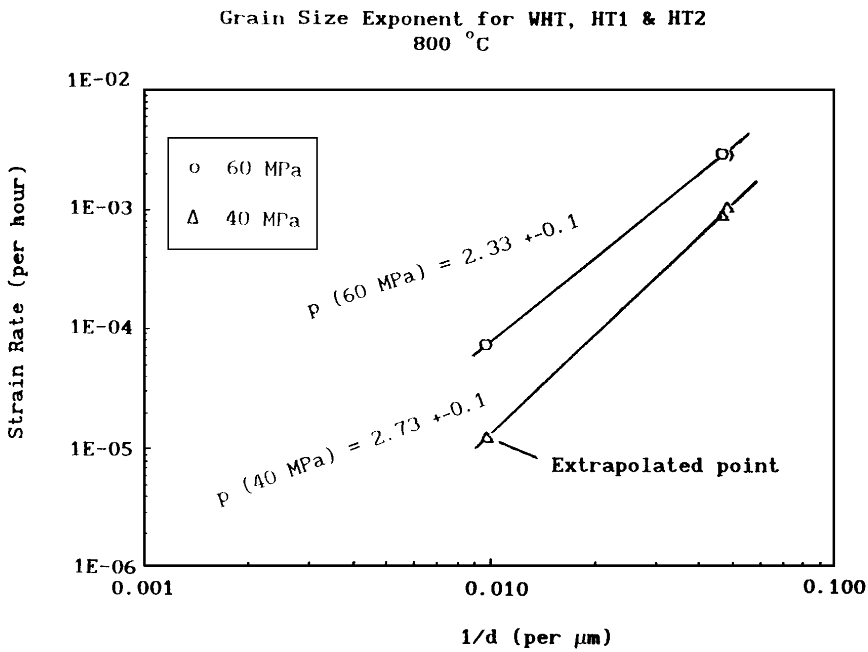

Figure 8. Steady state strain rate vs. $1/d$ for different heat treatments and $T = 800°C$. *Note:* Steady state strain rate at 40 MPa is extrapolated from figure 3.

3.4.2. Time to fracture. The dependence of time to fracture as a function of applied engineering stress for different heat treatments at a temperature of 800°C is illustrated in figure 9. These results were compared with the data obtained from Ref. [7], which produced Ni_3Al without boron by casting and used a test temperature of 815°C.

HT2 treatment gave a time to fracture longer than the other heat treatments. It can be also seen that up to 100 hours, the HT2 gives less time than Ref. [7]. After 100 hours, HT2 gives a longer time.

It is clear that the improved creep behaviour depends on the grain size. An increase of the grain size leads to an improvement of the creep behaviour. This is due to the fact that creep fracture occurs around the grain boundary [11, 12].

3.4.3. Ductility. Figure 10 shows the influence of the applied engineering stress on the percentage elongation. From this alloy, it is clear that the HT1 treatment has the highest value of the percentage elongation compared to the other heat treatments.

3.5. Larson-Miller parameter

The relationship between applied engineering stress and Larson-Miller parameter for different heat treatments is illustrated in figure 11. It is apparent that HT2 and HT3 are better heat treatment compared with other heat treatments.

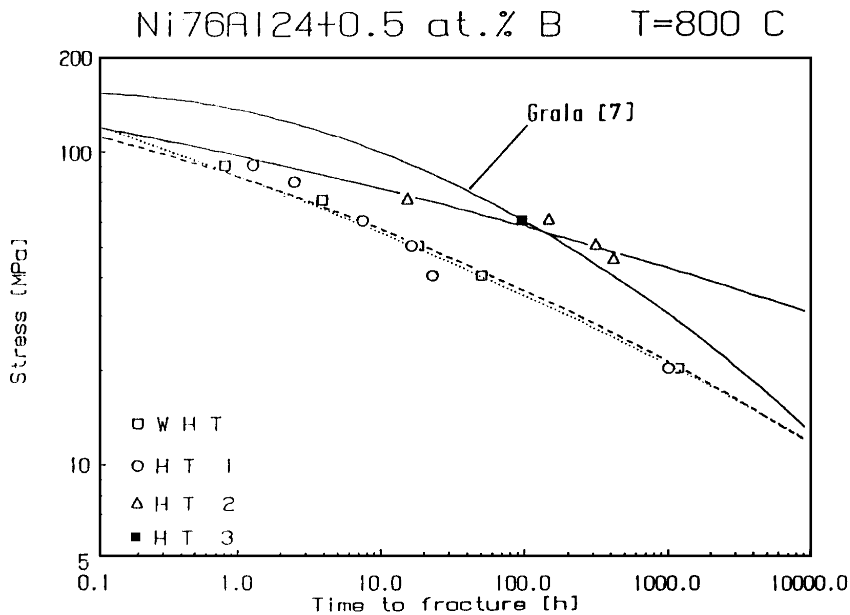

Figure 9. Applied engineering stress vs. time to fracture for different heat treatments and data obtained from Ref. [7].

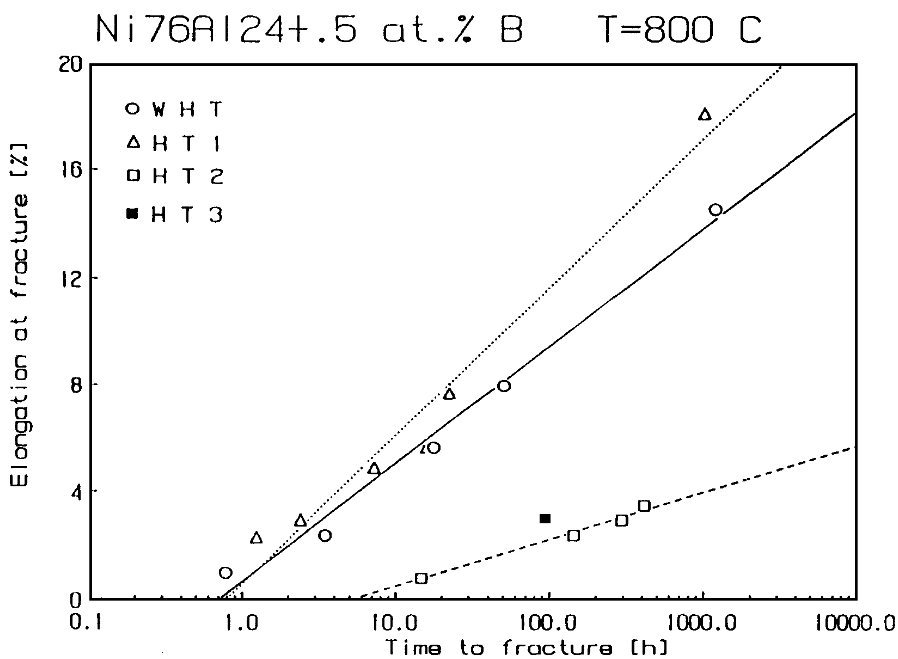

Figure 10. Percentage elongation at fracture vs. time to fracture for different heat treatments and $T = 800°C$.

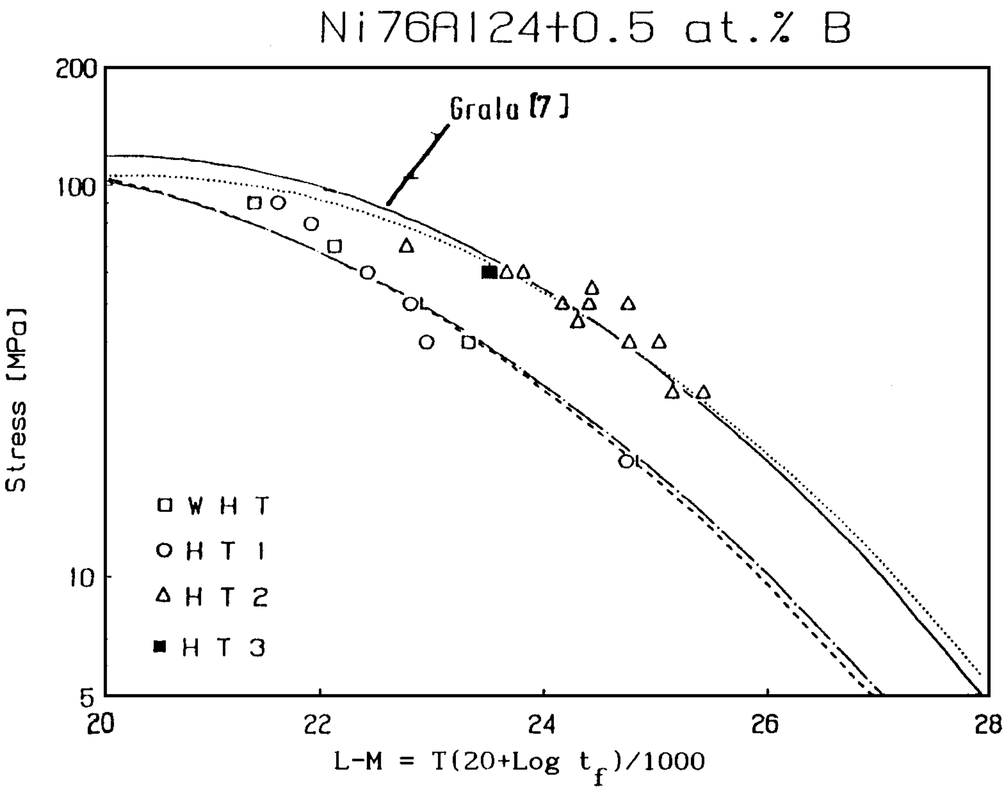

Figure 11. Applied engineering stress vs. Larson-Miller parameter for different heat treatments and data obtained from Ref. [7].

A comparison of the creep behaviour at 800°C for WHT and HT1 shows that its creep behaviour is not greatly different. This is attributed to the fact that a subsequent heat treatment has no effect on the grain size. On the other hand, the HT2 and HT3, which give increased grain sizes, yields better creep behaviour than WHT and HT1.

Comparison of the data of Ni_3Al reported in Ref. [7] with the data obtained in this work are represented in figure 11 as a relation between creep stress and Larson-Miller parameter. It is apparent that the Ni_3Al with boron (HT2 and HT3) is very closed of the Ni_3Al without boron produced as casting from Ref. [7].

3.6. Optimised heat treatment

As mentioned previously, its clear that HT2 and HT3 are the optimal heat treatments. The homogenization of the alloy at WHT and HT1 produced no visible change in grain size (figure 1). On the other hand, the homogenization of HT2 and HT3 led to an increase in the grain size, thus improving creep behaviour. For example, the time to fracture was increased from an average of 10 hours ($\dot{\varepsilon}_{ss} \cong 3 * 10^{-3}$ 1/h) for specimens from heat treated according to WHT and HT1 to approximately 141 and 100 hours ($\dot{\varepsilon}_{ss} \cong 7 * 10^{-5}$ and $1.4 * 10^{-4}$ 1/h) for specimen heat treated HT2 and HT3 respectively at the same conditions (60 MPa and 800°C).

4. Summary and conclusions

The creep behaviour of Ni_3Al with boron additions has been studied in the temperature range 800 to 900°C at different stress levels. A reliable set of data for power law creep of specimens were different heat treatments has been obtained. The stress exponent was dependent on the test temperature and the heat treatment conditions. The grain size exponent was calculated and shown to affect the creep behaviour. The mean apparent activation energy for creep was approximately 400 kJ/mol. The creep properties of this alloy were the most sensitive to grain size differences produced by the various heat treatments. The optimum heat treatment exhibiting the best creep behaviour was HT2 (1120°C/4 hours). So that the nickel aluminide with boron as a material for jet turbine engine components application can be consedered.

Nomenclature

a: Material constant
A: Percentage elongation, %
d: Grain size area, μm^2
E: Modulus of elasticity, MPa
HT: Heat treatment
n: Stress exponent
L-M: Larson-Miller parameter
p: Grain size exponent
Q: Apparent activation energy for creep, kJ/mol
R: Gas constant, J/K · mol
t_f: time to fracture, hour
T: Test temperature, K
WHT: without heat treatment
$\dot{\varepsilon}_{ss}$: steady state strain rate, 1/h
σ: Applied engineering stress, MPa

References

1. Westbrook, J.H.: Mechanical properties of intermetallic compounds. A Symp. Held During the 115th Meeting of the Electrochemical Soc. at Philadelphia, Pennsylvania, May 3–7, 1959, pp. 1–70.
2. Flinn, P.A.: Theory of deformation in superlattics. Trans. of Metall. Soc. of AIME, 218:145–154, 1960.
3. Liu, C.T., White, C.L., and Horton, J.A.: Effect of boron on grain-boundaries in Ni_3Al. Acta Metall., 33:213–229, 1985.
4. Aoki, K. and Izumi, O.: Nippon Kinzaku Gakkaiski, 43:1190–1196, 1979.
5. Liu, C.T. and Kock, C.C.: Technical aspects of critical materials used by steel industry. National Bureau of Standards, Washington, DC, 1983, Vol. IIB.

6. Sikka, V.K.: Advances in processing techniques for nickel aluminide. Advanced Materials and Processing Techniques for Structural Applications, Paris, France, Sept. 7–9, 1987, pp. 295–305.
7. Grala, E.M.: Investigation of NiAl and Ni_3Al. A Symp. held during the 115th meeting of the Electrochemical Soc. at Philadelphia, Pennsylvania, May 3–7, 1959, pp. 358–404.
8. Evans, R.W. and Wilshire, B.: Creep of metals and alloys. Preditive and Quantitives Metallurgy Series, D. McLear, Dotesio, Printers Ltd., England, 1985.
9. Langdon, T.G.: Deformation of polycrystals: Mechanisms and microstructures. Proc. 2nd Riso Int. Symp. on Metallurgy and Materials Science, N. Hansen et al., Riso National Laboratories, Roskilde, Denmark, 1981, pp. 45–54.
10. El-Magd, E.: Mechanisches Verhalten Metallischer Werkstoffe unter Berueksichtigung der Betriebsdingungen, Vorlesung des LFW, RWTH Aachen, 1989.
11. Stoloff, N.S.: Ordered for high temperature applications. Mat. Res. Soc. Symp. Proc., 39:3–27, 1985.
12. Destefani, J.D.: Advances in intermetallics. Advanced Material & Processes, 2(89):37–41.